SF2A 2007
J. Bouvier, A. Chalabaev, C. Charbonnel (eds)

ANALYTICAL CONSIDERATIONS OF SPACE DEBRIS WITH HIGH AREA-TO-MASS RATIOS LOCATED NEAR THE GEO REGION

S. Valk[1] and A. Lemaître[1]

Abstract. This paper provides a hamiltonian formulation of the averaged equations of motion with respect to short periods (1 *day*) of a space debris subjected to direct solar radiation pressure and orbiting near the geostationary ring. This theory is based on a semi-analytical theory of order 1 regarding the averaging process, formulated using canonical and non-singular elements for eccentricity and inclination. The dynamical evolution of space debris released near the geostationary ring, with area-to-mass ratios (A/m) as high as 40 m^2/kg is analyzed within the framework of mid-term evolution ($\sim$ 1 *year*) as well as long-term evolution (several decades). We also analyze the coupling equations between the eccentricity and the inclination, considering a doubly averaged analytical model.

1 Introduction

Optical surveys for space debris performed by the European 1m telescope on Tenerife (Canary islands) have discovered a significant population of small-size objects with diameters as small as ten centimeters near the geostationary ring (GEO). These uncatalogued space debris have mean orbital motions of about 1 rev/day and sometimes present highly eccentric orbits with eccentricities as high as 0.55 (Schildknecht et al., 2005). These objects are probably the result of unknown fragmentations occurred near the geostationary ring, but the identification of such past events is complicated. Initially, (Liou & Weaver, 2004) suggested that some of the resulting fragments are characterized by high area-to-mass ratios compared to those of typical spacecraft and upper stages. As a consequence, they proposed a simple explanation to the astonishing discovery of high eccentricity objects: the solar radiation might induce such a particular dynamics on space debris with sufficiently high area-to-mass ratio. Indeed, a satellite or space debris exposed to solar radiation pressure undergoes a force that arises from the absorption or reflection of photons. In contrast to gravitational perturbations, the acceleration due to solar radiation pressure depends linearly on the area-to-mass ratio. Under such assumptions, space debris may be affected by significant large eccentricities as well as important inclinations. Recent numerical investigations were performed to put this assumption to the test (Liou & Weaver, 2004), (Anselmo & Pardini, 2005). In this framework, short-term as well as long-term evolutions of geosynchronous space debris were studied in detail. (Liou & Weaver, 2004) also proposed the source of such high area-to-mass ratios, namely thermal blankets or multi-layer insulation (MLI), which is made from Mylar®, Kapton® or Nomex®.
The topic specifically addressed in this paper is the development of simplified and non-singular analytical models describing the evolution of space debris related to high area-to-mass ratios. On a qualitative point of view, this analytical approach is highly informative to underline the main properties of such objects.

2 Analytical investigations

2.1 Non-singular elements

As the counterpart of equinoctial elements, Poincaré's variables are suitable for all eccentricities and inclinations associated with an elliptical orbit. In particular, they remain consistent even for null eccentricities and inclinations. Because they are canonical, this set is especially useful for treating orbit problems with Hamiltonian

[1] University of Namur, Département de Mathématique, Unité de Systèmes Dynamiques, 8, Rempart de la Vierge, B-5000, Namur, Belgium

dynamics. The Poincaré's variables are:

$$x_1 = \sqrt{2P}\sin p, \quad y_1 = \sqrt{2P}\cos p, \quad x_2 = \sqrt{2Q}\sin q, \quad y_2 = \sqrt{2Q}\cos q, \tag{2.1}$$

where the modified Delaunay's elements are defined by: $P = L - G$, $p = -\omega - \Omega$, $Q = G - H$, $q = -\Omega$. The variables (L, G, H) are the classical Delaunay's elements given by: $L = \sqrt{\mu\, a}$,$G = \sqrt{\mu\, a(1-e^2)}$, $H = \sqrt{\mu\, a(1-e^2)}\cos i$, ω denotes the argument of perigee, Ω the longitude of the ascending node, a is the semi-major axis, e the eccentricity and i the inclination. Finally, μ is the gravitational constant of the Earth.

2.2 *Expansion of the radiation pressure disturbing function*

The potential related to direct radiation pressure can be written:

$$\mathcal{H}_{rp} = C_r\, P_r\, \frac{A}{m}\frac{a_\odot^2}{r_\odot}\sum_{n=0}^{n_{max}}\left(\frac{r}{r_\odot}\right)^n \mathcal{P}_n(\cos\Psi), \tag{2.2}$$

where Ψ is the geocentric angle between the Sun and the space debris. $\mathcal{P}_n$ is the Legendre polynomial of degree n and $(X_\odot, Y_\odot, Z_\odot)$ are the rectangular coordinates of the unit vector pointing towards the Sun; C_r is the non-dimensional reflectivity coefficient (fixed to 1 further on in this paper) which depends on the reflective properties of the space debris surface; $P_r = 4.56\cdot 10^{-6}\ N/m^2$ is the radiation pressure per unit of mass for an object located at a distance of 1 AU; $a_\odot$ is a constant parameter equal to the mean distance between the Sun and the Earth, that is $a_\odot = 1\ AU$; $\mathbf{r}$ is the geocentric position of the space debris and $\mathbf{r}_\odot$ is the geocentric position of the Sun.
Using an expansion in powers of the eccentricity and of the inclination, typically up to order 10, and after convenient substitutions, the potential formulation of Eq. (2.2) may then be expressed in terms of entirely non-singular and non-dimensional variables (X_1, Y_1, X_2, Y_2):

$$\mathcal{H}_{rp} = \sum_{n=0}^{n_{max}}\mathcal{R}_n = \sum_{n=0}^{n_{max}}\frac{1}{L^{2n}}\sum_{j=0}^{N_n}\mathcal{A}_j^n(X_1, Y_1, X_2, Y_2, X_\odot, Y_\odot, Z_\odot)\,\mathcal{B}_j^n(\lambda). \tag{2.3}$$

In Eq. (2.3), $\mathcal{B}_j^n$ denote trigonometric functions with respect to the mean anomaly λ. $\mathcal{A}_j^n$ are polynomials in the non-dimensional rectangular coordinates of the Sun as well as the so-called rectangular *non-dimensional Poincaré's variables* (X_1, Y_1, X_2, Y_2) of the space debris:

$$X_1 = \sqrt{\frac{2P}{L}}\sin p, \quad Y_1 = \sqrt{\frac{2P}{L}}\cos p, \quad X_2 = \sqrt{\frac{2Q}{L}}\sin q, \quad Y_2 = \sqrt{\frac{2Q}{L}}\cos q. \tag{2.4}$$

For similar developments and further details, we refer to (Valk S. et al., 2007a), where a direct method for the expansion of the geopotential of the Earth and the expansion of the luni-solar perturbations in non-dimensional, non-singular and rectangular variables is presented with its effective implementation in computer algebra.

2.3 *Toy models*

On a qualitative point of view, it would be interesting to underline the main properties of objects with high A/m ratios using simplified equations. Such an approach is adopted in (Chao, 2006) where the coupling effects between the solar radiation pressure effects and the luni-solar attractions is considered. In this framework, the latter provides a detailed understanding of the long-term evolution of both eccentricity and inclination. Regarding our approach, we will focus our efforts on the radiation pressure without taking into account the coupling between the radiation and the luni-solar effects. Consequently, this analysis will then emphasize the intrinsic effects related to radiation pressure. On the other hand, to avoid any singularity in eccentricity and inclination, the following simplified equations will be expressed using the before-mentioned non-singular set of variables.
As we are interested in the long-term dynamics, we average the disturbing function over the fast variable, namely the mean longitude λ. As a first approach, we average the disturbing function to the first order by dropping the fast periodic terms in the trigonometric functions. After isolating the dominant terms (first order approximation

in eccentricity and in inclination $\mathcal{O}(e, \sin i/2)$), and after using the non-dimensional ecliptic spherical coordinates $(\lambda_\odot, \beta_\odot)$ of the Sun instead of the rectangular coordinates $(X_\odot, Z_\odot, Z_\odot)$, the averaged potential takes the form:

$$\begin{aligned}\langle \mathcal{H}_{rp} \rangle_\lambda \quad = \quad & -\mathcal{Z}_1 \left\{ (C_\odot Y_1 - S_\odot X_1) \left(1 - \tfrac{1}{4}\,(X_2^2 + Y_2^2)\right) \right. \\ & \qquad \left. + \tfrac{1}{4} \left[(Y_2^2 - X_2^2)\,(C_\odot Y_1 + S_\odot X_1) \right] - 2X_2 Y_2 (S_\odot Y_1 - C_\odot X_1) \right\} \\ & -\mathcal{Z}_2 \left\{ (C_\odot Y_1 + S_\odot X_1) \left(1 - \tfrac{1}{4}\,(X_2^2 + Y_2^2)\right) \right. \\ & \qquad \left. + \tfrac{1}{4} \left[(Y_2^2 - X_2^2)\,(C_\odot Y_1 - S_\odot X_1) \right] + 2X_2 Y_2 (S_\odot Y_1 + C_\odot X_1) \right\} \\ & -\mathcal{Z}_3 \left\{ S_\odot\,(Y_1 X_2 - X_1 Y_2) \right\} + \mathcal{O}(e^2, \sin^2 i/2),\end{aligned} \tag{2.5}$$

where $\mathcal{Z} = \frac{3}{2}\, a\, C_r\, P_r\, \frac{A}{m} \left(\frac{a_\odot}{r_\odot}\right)^2$, $C_\odot = \cos\lambda_\odot(t)$, $S_\odot = \sin\lambda_\odot(t)$, $\mathcal{Z}_1 = \mathcal{Z}\,\cos^2\frac{\epsilon}{2}$, $\mathcal{Z}_2 = \mathcal{Z}\,\sin^2\frac{\epsilon}{2}$, $\mathcal{Z}_3 = \mathcal{Z}\,\sin\epsilon$ and ϵ is the obliquity of the Earth on the ecliptic. Let us remark that further on, the relative motion of the Sun around the Earth will be assumed to be circular with a constant angular motion of $n_\odot = 2\pi/[year]$.

Mid-term evolution of eccentricity and longitude of perigee: Considering the hamiltonian disturbing function defined in Eq. (2.5), the equations of variation are known, in particular in the eccentricity related variables (X_1, Y_1). These equations can be further reduced by neglecting the first and second order terms in (X_2, Y_2). Consequently, the are integrated with respect to time to obtain a *first order solution*:

$$\begin{aligned} X_1(t) \quad &= \quad -\frac{\mathcal{Z}}{L\, n_\odot}\,\sin\lambda_\odot(t) \quad + \quad \beta_0, \\ Y_1(t) \quad &= \quad \frac{\mathcal{Z}\,\cos\epsilon}{L\, n_\odot}\,\cos\lambda_\odot(t) \quad + \quad \alpha_0, \end{aligned} \tag{2.6}$$

where (α_0, β_0) are constants of integration determined from initial conditions. These equations describe an ellipse with center coordinates (α_0, β_0). In addition to the choice of non-singular variables, this simplified analytical model differs from the one developed by (Chao & Baker, 1983) by the presence of the term in $\sin^2\epsilon/2$. Neglecting the terms in $\sin^2\epsilon/2$, the ellipse becomes a circle, the radius of which is $R = (1/L\, n_\odot)\,\mathcal{Z}\cos^2\epsilon/2$. Eqs. (2.6) show that the so-called *eccentricity vector* $(\mathbf{Y_1}, -\mathbf{X_1}) \simeq (\mathbf{e}\,\mathbf{cos}(\omega + \mathbf{\Omega}), \mathbf{e}\sin(\omega + \mathbf{\Omega}))$ moves along this circle (counter clockwise) at a constant rate $n_\odot = 2\pi/[year]$. As a consequence, the longitude of perigee ϖ librates (Fig. 1 [left]) or circulates (Fig. 1 [right]) about a fixed value which depends on the initial conditions in eccentricity e_0 and in longitude of perigee ϖ_0 as well as on the radius of the circle, that is a directly proportional function of the ratio A/m.

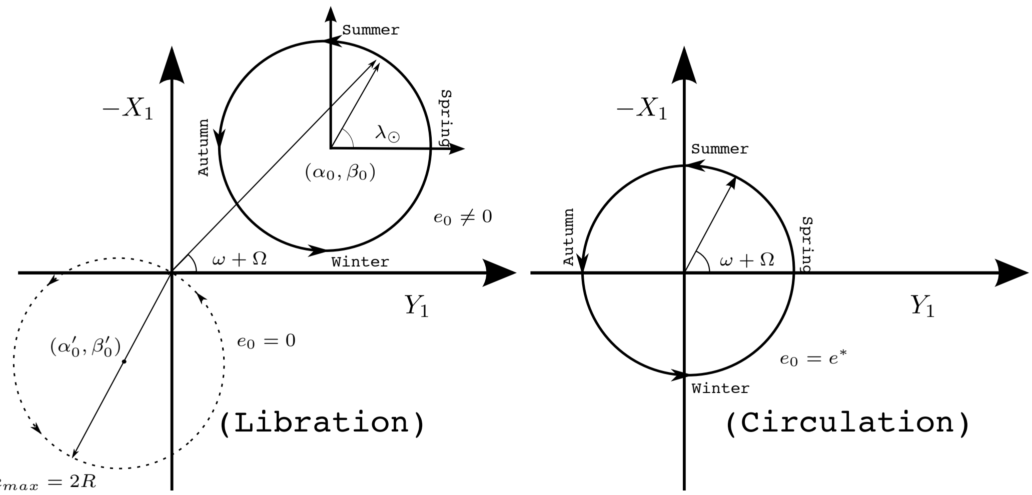

Fig. 1. Schematic mid-term evolution (yearly oscillations) of the eccentricity vector in the $(Y_1, -X_1) \simeq$ ($\mathbf{e}$ $\cos(\omega + \mathbf{\Omega}), \mathbf{e}$ $\sin(\omega + \mathbf{\Omega})$) phase space. Depending on the initial conditions in eccentricity e_0 and longitude of perigee ϖ_0, the longitude of perigee librates [left] or circulates [right] for a fixed value of the area-to-mass ratio A/m.

Long-term evolution of inclination and longitude of the ascending node: After substituting the first order approximation of the eccentricity and longitude of perigee variation defined by Eqs. (2.6) into the equations of variation of the inclination related variable (X_2, Y_2), one can define the doubly averaged equations with respect to the mean longitude λ and the ecliptic longitude $\lambda_\odot$, that is:

$$\begin{aligned} \left\langle \dot{X}_2 \right\rangle_{\lambda_\odot} &= \frac{\mathcal{Z}}{2\,n_\odot\,L^2}\left[(\mathcal{Z}_1-\mathcal{Z}_2)\,Y_2-\mathcal{Z}_3\right] = \frac{1}{2\,n_\odot\,L^2}\left[\mathcal{Z}^2\,\cos\epsilon\,Y_2-\mathcal{Z}\mathcal{Z}_3\right], \\ \left\langle \dot{Y}_2 \right\rangle_{\lambda_\odot} &= \frac{\mathcal{Z}\,\cos\epsilon}{2\,n_\odot\,L^2}\left(\mathcal{Z}_1+\mathcal{Z}_2\right)X_2 = -\frac{\mathcal{Z}^2\,\cos\epsilon}{2\,n_\odot\,L^2}\,X_2, \end{aligned} \tag{2.7}$$

where the relative motion of the Sun around the Earth is still assumed to be circular with a constant angular motion of $n_\odot = 2\pi/[year]$. This system of differential equations is no more and no less than a harmonic oscillator expressed in the rectangular coordinates X_2:

$$\left\langle \ddot{X}_2 \right\rangle_{\lambda_\odot} = -\nu_\Omega^2\,X_2 \qquad \text{with} \quad \nu_\Omega = \frac{\mathcal{Z}^2\,\cos\epsilon}{2\,n_\odot\,L^2}. \tag{2.8}$$

Moreover, a general solution of our second *simplified model* in inclination can be written as follows:

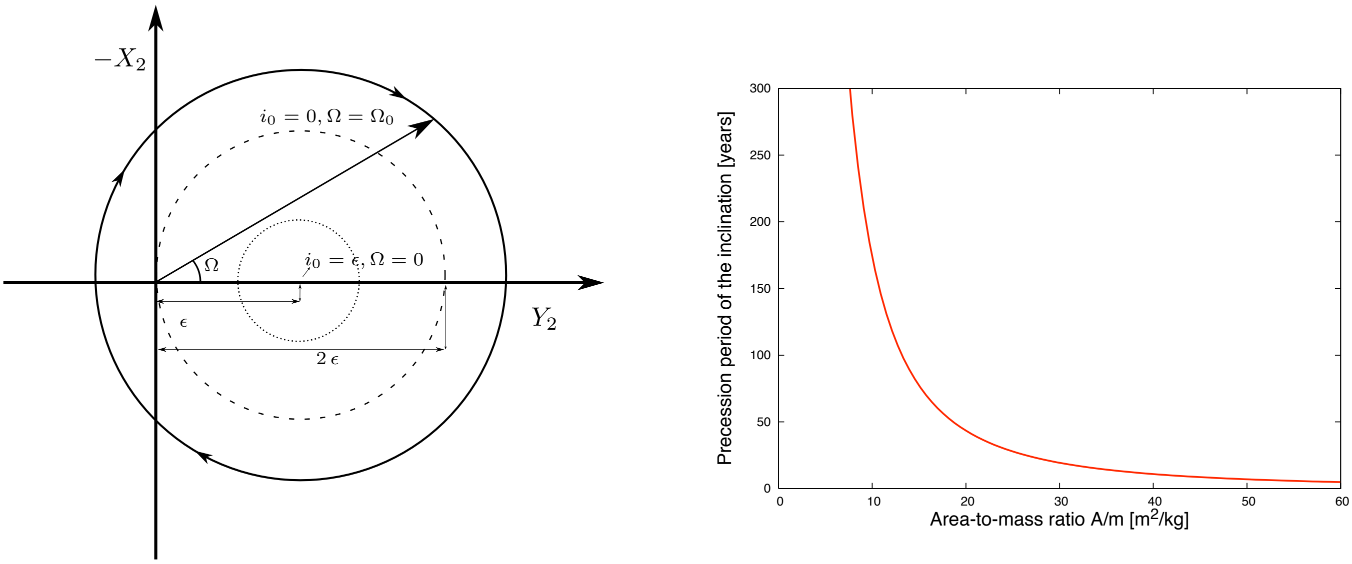

Fig. 2. Schematic long-term evolution of the inclination vector in $(Y_2, -X_2) \simeq (\sin i\,\cos\Omega, \sin i\,\sin\Omega)$ phase space [left]. Various regimes of the inclination vector are recognizable: *Circulation* (solid line) and *Libration* (dashed and doted line). Period of precession $2\pi/\nu_\Omega$ of the inclination vector with respect to the A/m [right].

$$\begin{aligned} \langle X_2 \rangle_{\lambda_\odot} &= -A_0\sin(\nu_\Omega t + \theta_0), \\ \langle Y_2 \rangle_{\lambda_\odot} &= \sin\epsilon - A_0\cos(\nu_\Omega t + \theta_0) + \mathcal{O}(\epsilon^2) \end{aligned} \tag{2.9}$$

where the amplitude A_0 and the phase difference θ_0 are determined from initial conditions. Eqs. (2.9) describe a circle with fixed center coordinates $(0, \sin\epsilon) = (0, \epsilon + \mathcal{O}(\epsilon^3))$ and a radius $R = A_0$. The so-called *inclination vector* $(\mathbf{Y_2}, -\mathbf{X_2}) \simeq (\sin\mathbf{i}\,\cos\mathbf{\Omega}, \sin\mathbf{i}\,\sin\mathbf{\Omega})$ moves along this circle (clockwise) at a constant rate ν_Ω. Similarly to the case of the eccentricity vector presented in Eqs. (2.6), the longitude of the ascending node will librate or circulate depending only on the initial conditions in inclination i_0 and longitude of the ascending node Ω_0. However, the libration regime takes place at about 0 degrees. On the other hand, the amplitude A_0 of the solution (2.9), that this the radius of the circle, is independent of the area-to-mass ratio as well as any multiplying factor present in the direct solar radiation pressure formulation. Indeed, the amplitude only depends on the initial conditions and on the obliquity ϵ of the Earth's orbit.
For the purpose of verifying the analytical results, we performed numerical integrations which use a home-made semi-analytical theory developed in non-singular variables (Valk S. et al., 2007a), (Valk S. et al., 2007b).

(Fig. 3 [left]) shows the mid-term evolution of the eccentricity. The amplitude of the mid-term oscillations, with a period of nearly one year, significantly grows with increasing area-to-mass ratio. Besides, (Fig. 3 [right]) shows that an increase of the area-to-mass ratio has as consequence a faster orbit pole precession. Moreover, we also see that the maximum amplitude of the inclination is independent of the A/m. These latter numerical results are in good agreement with (Liou & Weaver, 2004) and (Chao, 2006) and corroborate the dynamic behavior underlined by our simplified analytical models.

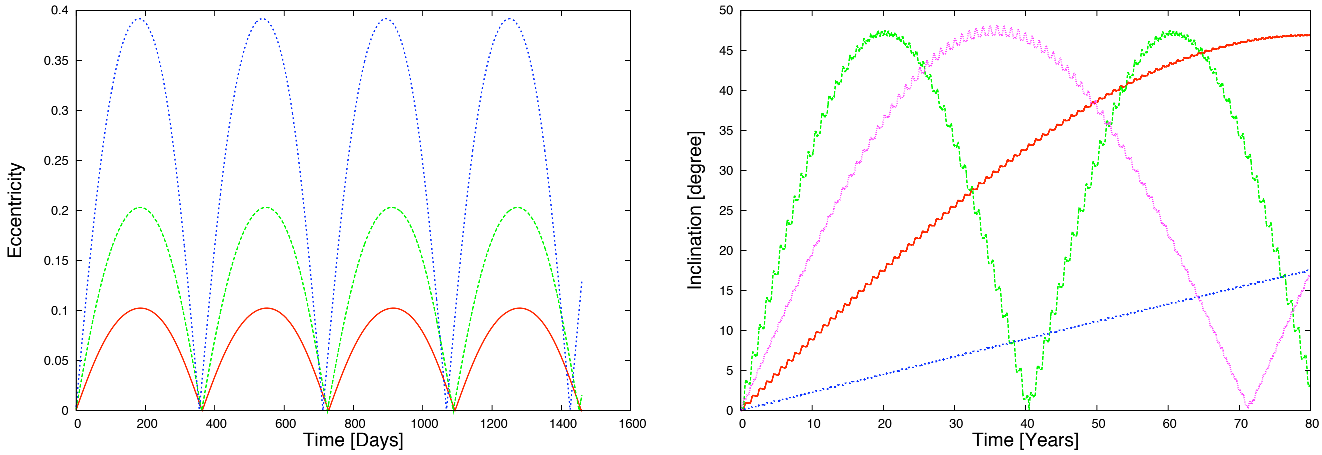

Fig. 3. Mid-term variations (yearly oscillations) of the eccentricity [left] and long-term variations of the inclination [right] as a function of various area-to-mass ratios ($A/m = 5, 10, 20\ m^2/kg$) for a fixed initial condition ($a_0 = 42164\ km, e_0 = 0, i_0 = 0\ rad, \omega_0 = \Omega_0 = \lambda_0 = 0\ rad$). Time at epoch is 21 March 2000.

Coupling equations between eccentricity and inclination: The equations of variation corresponding to the averaged potential defined in (Eq. 2.5) are not uncoupled in the set of variables (X_1, Y_1) and (X_2, Y_2), respectively. Consequently, it can be shown that the mid-term variations on the inclination related variables (X_2, Y_2) will induce additional long-term variations on the eccentricity vector by combination of mid-term periods only. The solution of this additional coupling effect between eccentricity and inclination can be written:

$$\begin{aligned} X_1(t) &= -\frac{\mathcal{Z}}{L\, n_\odot} \sin\lambda_\odot(t) + B_0 \sin(\nu_\Omega t + \phi_0), \\ Y_1(t) &= \frac{\mathcal{Z}\cos\epsilon}{L\, n_\odot} \cos\lambda_\odot(t) + B_0 \cos(\nu_\Omega t + \phi_0), \end{aligned} \tag{2.10}$$

Eqs. (2.10) show that the eccentricity vector always moves (counter clockwise) along a circle, defined in Eq. (2.6), the center of coordinates of which moves (clockwise) along a great circle of radius B_0 with a proper period of $2\pi/\nu_\Omega$. The combination of mid-term and long-term variations is illustrated schematically in Fig. 4 [left]. Using our semi-analytical theory, Fig. 4 [right] shows the evolution, over 40 *years*, of the eccentricity vector of a space debris, taking into account only direct solar radiation pressure. The pattern observed is, as expected, basically produced by the superimposition of two variations, the first with a period of 1 *year*, associated with the solution presented in Eq. (2.6), and the second with a period of many decades, that is the proper period $2\pi/\nu_\Omega$ of the longitude of the ascending node.

3 Conclusions

The mid-term and long-term evolution of the eccentricity and inclination vectors of geosynchronous space debris with high A/m ratios subjected to direct solar radiation pressure is analyzed using simplified models expressed in non-singular elements. The analytical investigations underline the main effects of the direct solar radiation pressure. These last results are also in good agreements with the works of (Chao, 2006) and (Anselmo & Pardini, 2005).

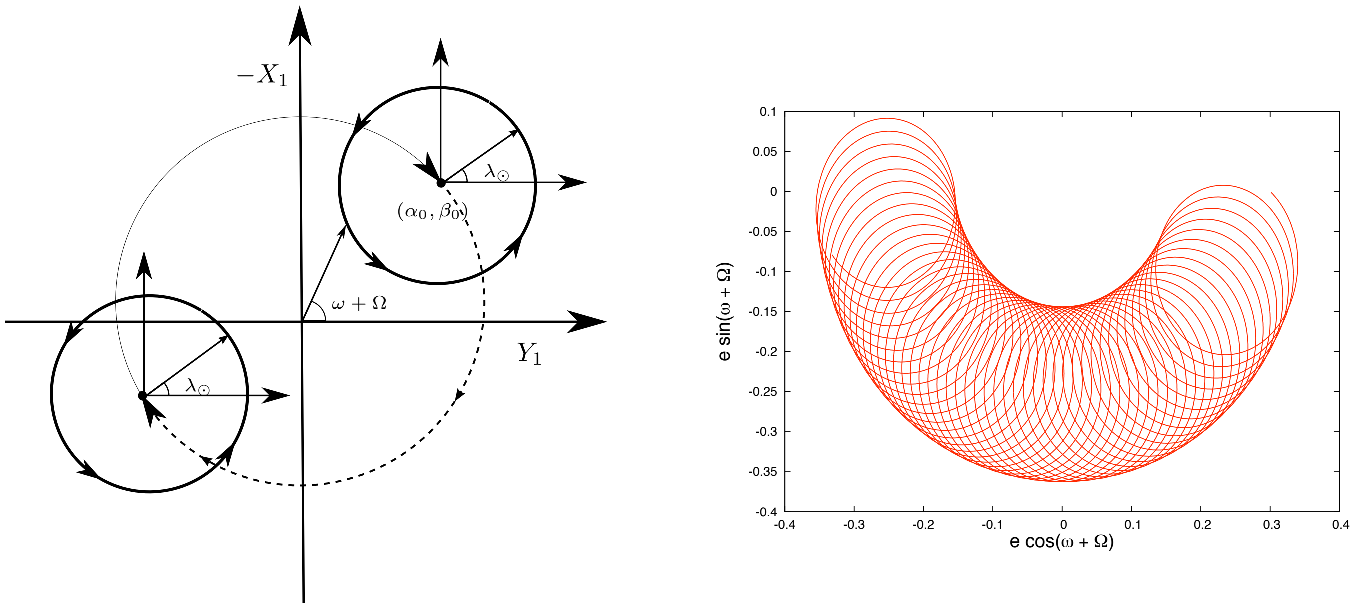

Fig. 4. Long-term and mid-term variations of the eccentricity vector coupled with the inclination and node revolution. Theoretical evolution in the $(Y_1, -X_1) \simeq (\, \mathbf{e}\ \cos(\omega + \mathbf{\Omega}), \mathbf{e}\ \sin(\omega + \mathbf{\Omega})\,)$ [left]. Numerical propagation over 40 *years* of a space debris projected in the $e\cos(\omega+\Omega), e\sin(\omega+\Omega)$ phase space [right]. Area-to-mass ratio and initial conditions are $A/m = 10\ m^2/kg$ and $(a_0 = 42164\ km, e_0 = 0.2, i_0 = 0, \omega_0 = \Omega_0 = M_0 = 0\ rad)$, respectively.

4 Acknowledgment

Part of this work was done in collaboration with the *Flight Dynamics Laboratory, Istituto di Scienza e Technologie dell'Informazione (ISTI), Consiglio delle Nazionale Ricerche (CNR), Pisa, Italy.* The authors thank Luciano Anselmo for helpful discussions and enlightening exchanges.

References

Anselmo L., Pardini C., Long-term evolution of High Orbits: Effects of Direct Solar Radiation Pressure and Comparison of Trajectory Propagators. *ISTI Technical Report 2007-TR-008*, PISA, Italy, 19 March 2007.

Anselmo L., Pardini C., Orbital Evolution of Geosynchronous Objects with High area-to-mass ratios. In Danesy, D. (Ed.), Proceedings of the Fourth European Conference on Space Debris, ESA SP-587, ESA Publications Division, Noordwijk, The Netherlands, pp. 279-284, August 2005.

Chao, C. C., Analytical Investigation of GEO Debris with High Area-to-Mass Ratio, AIAA Paper No. AIAA-2006-6514, Proceedings of the 2006 AIAA/AAS Astrodynamics Specialist Conference, Keystone, Colorado, August 2006.

Chao, C. C., Campbell, W. S., Long-term perigee height variations of GEO disposal orbits - A revisit, Proceedings of the 4th European Conference on Space Debris, Damrstadt, Germany, 18-20 April 2005.

Chao, C. C., Baker, J. M., On the propagation and control of geosynchronous orbits, Journal of the Astronautical Sciences, Vol. XXXI, No. 1, January-March 1983, pp. 99-115.

Chao, C. C., Applied orbit perturbation and maintenance, The Aerospace Press, American Institute of Aeronautics and Astronautics, 2005.

Liou J.-C, Weaver J.K., Orbital evolution of GEO debris with very high area-to-mass ratios, The Orbital Quarterly News, Vol. 8 issue 3, The NASA Orbital Debris Program Office, July 2004.

Schildknecht, T., Musci, R. Flury, W., Kuusela, J. de Leon, J. de Fatima Dominguez Palmero, L. Optical observations of space debris in high-altitude orbits, in Danesy, D. (Ed), Proceedings of the Fourth European Conference on Space Debris, ESA SP-587. ESA Publications Divison, Noordwijk, The Netherlands, pp. 113-118, 2005.

Valk S., Lemaître A., Deleflie F., Semi-analytical theory of mean orbital motion for geosynchronous space debris under gravitational influence, Submitted to Advances in Space Research, April 2007.

Valk S., Lemaître A., Anselmo L., Analytical and semi-analytical investigations of geosynchronous space debris with high area-to-mass ratios, Submitted to Advances in Space Research, June 2007.